AAPS PharmSciTech, Vol. 16, No. 3, June 2015 (© 2014)
DOI: 10.1208/s12249-014-0244-2

Research Article

Nanomicellar Topical Aqueous Drop Formulation of Rapamycin for Back-of-the-Eye Delivery

Kishore Cholkar,[1] Sriram Gunda,[1] Ravinder Earla,[1] Dhananjay Pal,[1] and Ashim K. Mitra[1,2]

Received 12 August 2014; accepted 23 October 2014; published online 26 November 2014

Abstract. The objective of this study was to develop a clear, aqueous rapamycin-loaded mixed nanomicellar formulations (MNFs) for the back-of-the-eye delivery. MNF of rapamycin (0.2%) was prepared with vitamin E tocopherol polyethylene glycol succinate (TPGS) (Vit E TPGS) and octoxynol-40 (Oc-40) as polymeric matrix. MNF was characterized by various parameters such as size, charge, shape, and viscosity. Proton nuclear magnetic resonance (^{1}H NMR) was used to identify unentrapped rapamycin in MNF. Cytotoxicity was evaluated in human retinal pigment epithelial (D407) and rabbit primary corneal epithelial cells (rPCECs). *In vivo* posterior ocular rapamycin distribution studies were conducted in male New Zealand white rabbits. The optimized MNF has excellent rapamycin entrapment and loading efficiency. The average size of MNF was 10.98±0.089 and 10.84±0.11 nm for blank and rapamycin-loaded MNF, respectively. TEM analysis revealed that nanomicelles are spherical in shape. Absence of free rapamycin in the MNF was confirmed by ^{1}H NMR studies. Neither placebo nor rapamycin-loaded MNF produced cytotoxicity on D407 and rPCECs indicating formulations are tolerable. *In vivo* studies demonstrated a very high rapamycin concentration in retina-choroid (362.35±56.17 ng/g tissue). No drug was identified in the vitreous humor indicating the sequestration of rapamycin in lipoidal retinal tissues. In summary, a clear, aqueous MNF comprising of Vit E TPGS and Oc-40 loaded with rapamycin was successfully developed. Back-of-the-eye tissue distribution studies demonstrated a very high rapamycin levels in retina-choroid (place of drug action) with a negligible drug partitioning into vitreous humor.

KEY WORDS: back-of-the-eye; drug delivery; formulation; mixed nanomicelles; posterior; rabbits; rapamycin/sirolimus; retina/choroid; sclera; topical eye drops.

INTRODUCTION

Posterior segment ocular diseases include non-infectious posterior uveitis (NIU), age-related macular degeneration (AMD), choroidal neovascularization (CNV), retinal neovascularization, posterior vitreoretinopathy (PVR), diabetic retinopathy, and cystoid macular edema. NIU affects patients of different age groups and it may be chronic and recurrent (1). However, management of NIU is far more challenging than anterior uveitis which leads to irreversible vision loss/impairment. Immediate and vigorous response (immunological and inflammatory) against ocular antigens is still unclear. Lymphocytes can stimulate ocular autoimmune activity in response to Th1 or Th17 (2). A major aim of NIU management includes suppression of inflammation and diminution of NIU intensity (3). The first class of FDA-approved drugs for treating NIU are corticosteroids (4). Both systemic and local ocular corticosteroid administrations are commonly indicated in NIU, particularly in patients who can tolerate steroid side effects. Alternatively, immunomodulation is a second-line choice of NIU treatment. Immunomodulators such as rapamycin (sirolimus), tacrolimus, and cyclosporine-A help to lower steroid-induced side effects such as cataract development, glaucoma, proliferative vitreoretinopathy, cystoid macular edema, vascular occlusion, and blindness (5).

Other diseases affecting the back-of-the-eye include neovascularization. In this disease condition, new leaky and fragile blood vessels are developed. The new vasculature branches out from the choroid and then grows through Bruch's membrane into sub-retinal pigment epithelia. Further, this new vasculature causes capillaries to leak causing blood and fluid accumulation in the retinal layers. During neovascularization, vascular endothelial growth factor (VEGF) is upregulated (6). Increased production of VEGF is induced by multiple cellular pathways: (i) hypoxia and (ii) pro-inflammatory cytokines such as TNF-α and β2 (7,8).

Anti-angiogenic agents can minimize neovascularization. Photosensitizing drugs such as verteprofin, lutetium, texaphyrin, and tin ethyl etiopurpurin have also been indicated in neovascularization (9–11). Use of laser light is expensive, require a medical specialist, and may leave a scar after treatment. Treatment of ocular neovascularization by

[1] Division of Pharmaceutical Sciences, School of Pharmacy, University of Missouri—Kansas City, 5258 Health Science Building 2464 Charlotte Street, Kansas, Missouri 64108, USA.
[2] To whom correspondence should be addressed. (e-mail: mitraa@umkc.edu)

macromolecular VEGF inhibitors such as pegatanib and ranibizumab has been approved for intravitreal use in CNV patients. Also, bevacizumab is widely used in CNV treatment. An investigational comparative study by Stalh *et al.* between the VEGF inhibitors and rapamycin suggested that rapamycin is more potent than VEGF inhibitors and alters response of the endothelial cells to the VEGF stimulation (12). Inhibitory effects of rapamycin are observed to check apoptosis. It also activates metalloproteins, promoting metastatic tumor growth, angiogenesis, and upregulation of interleukin-1 transcription and cAMP levels. Rapamycin is also a functional cytokine antagonists and more potent than cyclosporine (13).

Rapamycin or sirolimus is produced by *Bacterium Streptomyces Hygroscopicus*. Rapamycin acts by binding to FK-binding protein 12 (FKBP protein) in the cytosol forming a complex. Further, this complex binds to mammalian target of rapamycin receptor (mTOR) (14). Rapamycin generates its anti-inflammatory activity by inhibiting progression of cell cycle from G1 phase to S phase in T cells by blocking interleukin-2-mediated signal transduction pathway. In general, rapamycin mutes the responses of T and B cells induced by both calcium-dependent and calcium-independent stimuli (13,15). This agent exhibits multiple mechanisms of action other than anti-inflammatory property. It also exhibits anti-angiogenic, antifibrotic, antifungal, and antimigratory mechanisms (12,16–19). Rapamycin decreases VEGF production and alters the response of endothelial cells to VEGF stimulation (12).

Rapamycin is extremely hydrophobic with an octanol/water partition coefficient (log P) of 5.77 and an aqueous solubility of 2.6 μg/mL (20). Also, rapamycin is pH and light sensitive (21). Oral or intravenous administration of rapamycin for back-of-the-eye delivery is not medically acceptable. Rapamycin, an immunosuppressant, may severely compromise immune function if administered through systemic route (22). To deliver rapamycin locally to the eye, various strategies such as route of administration (periocular, subconjunctival, intravitreal implants/injections), and formulations (nanoparticles, liposomes) based have been implemented (1,20,23). Strategies such as periocular, subconjunctival, and intravitreal implants/injections of rapamycin are invasive and associated with side effects such as retinal detachment or damage, endophthalimitis, and pseudoendophthalmitis. Polyethylene glycol-b-poly(e-caprolactone) micelles have been previously developed to improve solubility. This micellar formulation resulted in an improvement of solubility up to a concentration of 1 mg/mL (24).

Among the ocular delivery routes, topical drop instillation is the most patient-acceptable route of drug administration. Static and ocular barriers impede drug permeation from the front to the back-of-the-eye tissues (retina/choroid). Therefore, the objectives of this work is to improve rapamycin aqueous solubility, develop a novel clear, aqueous, mixed nanomicellar formulation (MNF), and deliver therapeutic rapamycin levels in the back-of-the-eye tissues with topical drop instillation. To achieve this objective, we have employed a blend of polymers (vitamin E tocopherol polyethylene glycol succinate-1000 (Vit E TPGS) and octoxynol-40 (Oc-40)). Vit E TPGS is a FDA-approved amphiphilic polymer. In the pharmaceutical industry, it is employed as an emulsifier, solubulizer, absorption enhancer, and vehicle for hydrophobic drugs (25). Vit E TPGS has a hydrophilic liphophilic balance (HLB) value of 13.0 and critical micellar concentration of 0.02 wt% (26). This HLB value renders it to be a more lipophilic polymer relative to the second polymer (octoxynol-40). Also, Vit E TPGS is a potent inhibitor of multi-drug efflux pumps (P-glycoprotein, P-gp), facilitates drug translocation across cell membrane, modulates drug pharmacokinetics, and improves bioavailability (27,28). Another polymer, Oc-40 employed in this study, is also FDA-approved for human use. It has a HLB value of 18.0 which makes it a hydrophilic polymer. A unique ratio of these polymeric blend (4.5:2.0, for Vit E TPGS and Oc-40) was selected due to their low critical micellar concentration (0.012 wt%) of the combination relative to individual polymers (29,30). Further, this formulation has been characterized and evaluated for toxicity on rabbit primary corneal epithelial cells and human retinal pigment epithelial cells. Moreover, we have determined that mixed nanomicellar carrier has the ability to deliver rapamycin to the back-of-the-eye tissues from topical drop instillation.

Materials

Rapamycin was obtained from LC labs, USA. Vitamin E TPGS was purchased from Peboc division of Eastman Company, UK Limited, UK. Igepal (octoxynol-40) was obtained from Rhodio Inc., New Jersey, USA. Kollidon(R) 90F (povidone K 90) Ph. Eur., USP was procured from Mutcher, Inc., Pharmaceutical ingredients, Harrington Park, New Jersey, USA. HPLC grade methanol and acetonitrile were procured from Fisher Scientific, USA. Ethanol was purchased from Aaper alcohol and chemical Co. Shelbyville, Kentucky, USA. For all the formulation preparations, HyClone cell culture water, HyClone, USA, was utilized.

Cell Culture

Rabbit corneal epithelial cells (rPCECs) were cultured according to a previously published protocol from our laboratory (31). In brief, rPCECs were grown with culture medium comprising MEM, $NaHCO_3$, 10% FBS, HEPES, sodium bicarbonate, penicillin, streptomycin sulfate, and 1% (*v/v*) nonessential amino acids, adjusted to pH 7.4. Cells in passage numbers between 4 and 9 were selected for these experiments. Human retinal pigment epithelial cells (D407) were grown in a culture medium containing DMEM supplemented with 10% (*v/v*) FBS (heat-inactivated), 29 mM $NaHCO_3$, 15 mM HEPES, 100 mg of penicillin and streptomycin each, and 1% nonessential amino acids at pH 7.4. Cells in passage numbers between 75 and 80 were employed. Cells were grown at 37°C, in a humidified atmosphere of 5% CO_2 and 90% relative humidity. The growth medium was changed every other day for both cell lines. rPCEC and D407 cells were cultured in flasks, harvested at 80–90% confluency with TrypLE™ Express (a superior replacement for trypsin) (Invitrogen, Carlsbad, CA, USA). Cells were then plated in 96-well plates at a density of 10,000 cells/well and utilized for studies.

Method of Preparation

Rapamycin-loaded mixed nanomicellar formulations (MNFs) were prepared by a novel solvent evaporation method as described in previously reported procedure (29). Briefly, MNF (10 mL) was prepared by dissolving vitamin E tocopherol polyethylene glycol succinate (Vit E TPGS) (450 mg) and

octoxynol-40 (Oc-40) (200 mg) separately in absolute ethanol. Rapamycin was accurately weighed and dissolved separately in absolute ethanol. Vit E TPGS and Oc-40 solutions were mixed together to obtain a clear homogeneous solution. To this mixture, varying concentrations of rapamycin (dissolved in ethanol) were added to generate an overall concentration of 1 and 2 mg/mL in the final formulation. The mixture was stirred well which resulted in a clear solution. Solvent was evaporated by rotary evaporator and the formulation was vacuum-dried overnight to obtain a dried film. This thin film was then hydrated with HyClone water and resuspended to obtain a clear solution. Addition of water spontaneously generated rapamycin-loaded mixed nanomicelles. Sonication was applied for 20 min and final volume of the formulation was made up with 2X phosphate buffer (pH=6.8±0.1). A viscosity enhancer povidone K 90 was added to all the formulations. This formulation was filtered through 0.2-μm nylon membrane to remove any foreign particulate matter. A blank formulation was also prepared following a similar procedure described above without rapamycin.

Characterization of Mixed Nanomicellar Formulation

Optical Clarity. The optical clarity of prepared formulations was measured with UV-visible spectrophotometer (model: Biomate-3, Thermo Spectronic, Waltham, MA). A sample volume of 500 μL was taken for each analysis. HyClone cell culture water served as blank.

Viscosity. Viscosity of placebo and rapamycin-loaded MNF was adjusted with povidone K 90 employing Ostwald-Cannon-Fenske viscometer. The viscometer was filled from one end with ~5 mL MNF with extreme care to avoid air bubble formation. The solution was aspirated from the other end. Time taken by the MNF to flow down under gravity was measured. Density for MNF was also determined. Viscosity of the MNF was determined by comparing with water. Equation 1 was applied to determine the viscosity of MNF.

$$\text{Viscosity}_{(\text{MNF})} = \frac{\left(\text{density}_{(\text{MNF})} * \text{time}_{(\text{MNF})} * \text{viscosity}_{(\text{water})}\right)}{\left(\text{density}_{(\text{water})} * \text{time}_{(\text{water})}\right)} \quad (1)$$

Osmolality and pH. All prepared formulations were examined for osmolality and pH. For measurement of osmolality, an advanced osmometer (Model 3D3, Two Technology way, Norwood, Massachussets, USA) was utilized. A sample volume of 400 μL was used to measure osmolality. The pH of all formulations was measured with a Oakton pH meter (model: pH 510 series, Oakton Instruments, Vernon Hills, IL).

Size, Polydispersity Index, and Surface Potential

The mean hydrodynamic nanomicellar size, distribution, PDI, and surface potential of MNFs were measured by dynamic light scattering (DLS) (Brookhaven Instruments Corporation, Austin, TX, NY). DLS is a non-destructive technique to measure the molecule/particle size in submicrons level, at a laser wavelength of 659.0 nm and temperature of 25°C. A sample volume of 500 μL was used for size, distribution, and PDI. A volume of 1000 μL was utilized for surface potential measurement. The average values of three micellar diameter measurements of 12 runs were calculated for all samples.

Transmission Electron Microscopy

To determine shapes, surface morphology, and real-time size of rapamycin-loaded MNF, scanning transmission electron microscope CM12 (STEM) was utilized. To visualize mixed nanomicelles with STEM, negative staining was applied with uranyl acetate.

RP-HPLC Method

To determine concentration of entrapped drug within the core of MNF, reversed-phase (RP)-HPLC analysis was performed utilizing C8 column (Phenomenex C8, 5 μm; 150 mm × 2.1 mm), an autosampler (Alcott, model 718 AL), a column heater (Flatron CH-30 column heater, Flatron Systems Inc., USA) set at 40°C, a pump (model SD 20, shimadzu) set to deliver 1.0 mL/min, a UV detector (Shimadzu, SPD 20A) set at 278 nm, and an integrator to collect data. The mobile phase comprised of acetonitrile-methanol-water (30:35:35 *v/v/v*). Since the mobile phase contained higher organic phase, it was prepared freshly before analysis. A 50-μL sample was injected into the HPLC system.

Entrapment and Loading Efficiency

In the present study, the total amount of rapamycin entrapped in MNFs was determined by RP-HPLC. One milliliter of each MNF sample was collected into 1.5-mL micro centrifuge tubes and centrifuged at 10,000 rpm for 10 min at 4°C. Approximately 0.5 mL of supernatant was carefully collected into a fresh tube and lyophilized to obtain a solid pellet. This pellet was resuspended in 0.5 mL of dichloromethane (an organic solvent) that resulted in a clear solution. Due to addition of dichloromethane, rapamycin was released in the surrounding organic environment due to orientation reversal of hydrophobic and hydrophilic segments to form reversed micelles (32). The solution was evaporated under a speed vac (Genevac Technologies VC3000D speed vacuum, USA) to obtain a solid pellet. The solid pellet was diluted with HPLC mobile phase, and the amount of drug present in the diluted sample was determined. The amounts of rapamycin in the core of micelles were calculated by subtracting the total amount of unentrapped drug. The percent entrapment and loading efficiency of rapamycin were calculated according to Eqs. 2 and 3, respectively.

$$\text{Percent drug entrapped} = \frac{\text{mass of rapamycin in nanomicelles} * 100}{\text{mass of rapamycin added in formulation}} \quad (2)$$

$$\text{Loading efficiency} = \frac{\text{mass of rapamycin in nanomicelles} * 100}{\text{mass of rapamycin added} + \text{mass of polymers added}} \quad (3)$$

^{1}H NMR Characterization

To determine the presence of free rapamycin in solution, qualitative analysis was conducted with proton nuclear magnetic resonance (^{1}H NMR). Studies were performed for rapamycin, blank MNF, and rapamycin-loaded Vit E TPGS/Oc-40 MNFs. ^{1}H NMR spectra were recorded on a Varian 400 MHz spectrometer (Varian, USA) in deuterated water (D_2O) or deuterated chloroform ($CDCl_3$) at room temperature.

Dilution Stability

To study the effect of dilution on the MNFs, samples were diluted from 0 to 100 times with distilled water. The concentration of the monomers was well above the CMC (0.012 wt%). After dilution, micelle size was determined with DLS instrument.

Cytotoxicity Studies

To evaluate toxicity of MNFs, lactate dehydrogenase (LDH) release was conducted on rabbit primary corneal epithelial cells (rPCECs). Also, toxicity was evaluated on rPCEC and D407 with WST-1 cell proliferation assay. Rapamycin MNF has been prepared and evaluated for topical ocular delivery. Following topical drop administration, MNF primarily bathes the corneal epithelial cells. Therefore, we proposed to test the effect of MNF on both rPCEC and D407 cells.

Cell Proliferation Assay. Cell viability assay was performed to determine the toxicity of rapamycin MNF on rPCEC and D407 cells. Briefly, for these experiments 10,000 cells/well were placed into 96-well plates and exposed to 100 μL of placebo (blank) and 0.2% rapamycin-loaded MNFs for 1 h. MNFs (blank and rapamycin-loaded) were prepared in serum-free cell culture media and filtered through 0.22-μm sterile nylon membrane filters under laminar flow. In these experiments, cell culture medium and 10% triton X-100 served as negative and positive controls, respectively. Viable cells percentage was calculated considering the medium as 100%. Premixed WST-1 cell proliferation reagent was added according to the manufacturer's protocol (Clontech, Mountain View, CA). Cell proliferation assay is based on the enzymatic cleavage of tetrazolium salt (WST-1) to a water-soluble formazan dye, which is detected by absorbance at 450 nm with a micro titer plate reader (Analyst GT, Molecular Devices, Sunnyvale, CA). The amount of formazan formed is directly proportional to the number of viable cells. The percent cytotoxicity of the placebo and 0.2% rapamycin-loaded MNF were calculated.

LDH Assay. In vitro plasma membrane decay with blank and rapamycin-loaded MNFs was conducted on rPCECs and quantitatively measured with Takara Aqueous Non-Radioactive LDH cytotoxicity detection Kit (Takara Bio Inc, CA, USA). rPCECs were grown on 96-well plates as described previously (29). After 48 h of growth, rPCECs were added with 100 μL of serum-free cell culture medium; 100 μL of blank and rapamycin-loaded MNFs in serum-free culture media were added in each well and incubated for 2 h at 37°C. In this assay, cell culture media and 10% Triton-X100 served as negative and positive controls, respectively. After incubation, the plate was centrifuged at 250×*g* for 10 min in a dark condition. One hundred microliters of supernatant was transferred to an optically clear 96-well flat bottom plate and added with a solution containing equal volumes of catalyst and dye solution (prepared following manufacturer's protocol). This mixture was incubated for 15 min at room temperature in dark. The amount of formazan formed was measured with a 96-well micro titer plate reader absorbance set at 490 nm. A rise in reading number indicates increased LDH release in the culture medium which directly correlates with the amount of formazan produced. Therefore, the amount of formazan produced is proportional to the number of plasma membrane-damaged cells. Cytotoxicity was calculated according to Eq. 4.

$$\%\ \text{Cytotoxicity} = \frac{(\text{Observed experimental value} - \text{cell culture medium value}) * 100}{\text{Triton X} - 100 - \text{cell culture medium value}} \tag{4}$$

LC-MS/MS Method

A sensitive LC-MS/MS method was applied to determine the concentration of rapamycin in the back-of-the-eye tissue homogenates and fluids. LC-MS/MS is comprised of triple quadrupole mass spectrometer with electronspray ionization (ESI) on a turbo ionspray source (API 3200; Applied Biosystems, Foster City, CA, USA) which is coupled to a liquid chromatography system (Prominence HPLC shimadzu, Riverwood Drive, Columbia, Maryland, USA). A reversed-phase C8 column 5 μm, 50×4.6 mm (Waters, Corporation, USA), was selected for the separation and analysis of rapamycin with erythromycin as internal standard. The column temperature was maintained at 40°C. The mobile phase consisted of acetonitrile-water (80:20 *v/v*) with 0.1% formic acid and was pumped at a flow rate of 0.25 mL/min. Multiple reaction monitoring (MRM) mode was utilized to detect the compound of interest. A separate calibration curve (range of 3.5–1000 ng/mL) was constructed for the back-of-the-eye tissue (retina/choroid, sclera) and vitreous humor.

In Vivo Studies

Animals. New Zealand white male rabbits weighing between 2.0 and 2.5 kg were employed for *in vivo* studies. Animals were obtained from Myrtle's rabbitry (Thompson, TN) and acclaimed for 24 h in the animal care facility. Animal care and treatment in this investigation was in compliance with the Association for Research in Vision and Ophthalmology (ARVO) statement for the use of animals in ophthalmic and vision research.

Posterior Ocular Tissue Dissection

Animals were anesthetized prior to an experiment with ketamine HCl (35 mg/kg) and xylazine (3.5 mg/kg) administered intramuscularly. For the treatment, N=10, eyes were utilized. Anesthesia was maintained throughout the

experiment. Fifty microliters of 0.2% rapamycin MNF was instilled into each conjunctival sac. After a period of 60 min, euthanasia was performed under deep anesthesia with an intravenous injection of sodium pentobarbital through the marginal ear vein. Following euthanasia, the globe was immediately enucleated within a period of 2 min and was transferred to the ice cold Dulbecco's phosphate buffer saline (DBPS, pH=7.4). Enucleated eyes were rinsed twice in the ice cold DPBS to remove any traces of drug adsorbed onto the surface of the tissue. Aqueous humor was withdrawn using a 27-guage needle by limbal paracentesis. A small incision was made at the back of the globe and the vitreous humor was aspirated with the tuberculin syringe. Care was taken to avoid contamination by other tissues such as the lens. The lens was carefully separated and collected. The iris-ciliary body was removed and cornea was excised by incision along the sclera-limbus junction. Retina-choroid layer was removed and separated from the sclera. All the collected tissues were dried with Kimwipes®. Dissected posterior ocular tissues (sclera and retina-choroid) were transferred to preweighed eppendorf tubes and stored at −80°C until further extraction and analysis. Vitreous humor was transferred to a 15-mL falcon tube and stored at −80°C until further analysis.

Excised posterior ocular tissue (retina-choroid) was thawed. Five hundred microliters of chilled DPBS was added to retina-choroid. Similarly, sclera was thawed and 2.0 mL of chilled DPBS was added. The tissues were homogenized with a tissue homogenizer (Tissue Tearor, Model 985-370; Dremel Multipro, Racine, WI) in an ice bath for a period of 4 min. Vitreous humor was extracted and analyzed for rapamycin.

Drug Extraction. For rapamycin extraction, a volume of 200 μL of tissue homogenate was used. For vitreous humor, a volume of 100 μL was aspirated. Rapamycin was extracted from the back-of-the-eye tissues following a previously described protocol from our laboratory (33). Briefly, to extract rapamycin, protein precipitation method was used. To all the tissue homogenates, except blank, 25 μL of IS at a concentration of 5.0 μg/mL was added and vortexed for 1 min. Twenty-five microliters of 50% triethylamine in methanol (*v/v*) was added to all the samples and then vortexed vigorously for 2 min. Proteins were precipitated by addition of 800 μL of methanol. All the tissue homogenate samples were vortexed for another 2 min. Samples were centrifuged at 10,000 rpm for 30 min at 4°C. A volume of 500 μL supernatant was separated and evaporated using SpeedVac® (Savant Instruments, Inc, Holbrook, NY). One hundred microliters of HPLC mobile phase was added to the dry residue and reconstituted by vortexing for 2 mins. Further, this solution was centrifuged for 1 min at 1000 rpm and the supernatant was injected into HPLC for rapamycin quantification.

Statistical Analysis

Data for *in vitro* experiments were conducted at least in quadruplicate, and the results were expressed as mean±standard deviation (SD). Statistical comparison of mean values was performed with Student's *t* test. A *p* value of <0.05 was considered to be statistically significant.

RESULTS AND DISCUSSION

Rapamycin is a small molecule with poor aqueous solubility (2.6 μg/mL) (20). In the present study, we selected a blend of two FDA-approved polymers (Vit E TPGS and Oc-40) to entrap rapamycin into nanomicelles to improve its solubility. A weight percent ratio of 4.5:2.0 for Vit E TPGS and Oc-40 was selected due to their low critical micellar concentration (CMC) value of 0.012 wt% relative to individual polymers (Vit E TPGS (0.025%) and Oc-40 (0.107 wt%)) (29). Low CMC of this polymeric mixture allows to improve stability of MNF. In the present study, we successfully prepared 0.1 and 0.2% rapamycin-loaded MNFs with a blend of Vit E TPGS/Oc-40 (4.5:2.0) in phosphate buffer. Although, rapamycin solubility was improved with aqueous MNF, but topical drop instillation of aqueous drops may not retain the formulation in the pre-corneal pocket for longer period of time. A large portion (>90%) of the topically applied formulations is lost due to tear drainage, induced lacrimation, and tear dilution. Reflex blinking and loss of excess drop instillation may lead to spill over. Therefore, to improve MNF retention in the pre-corneal pocket viscosity enhancer with bio-adhesive properties is advisable. In the current study, we selected povidone K 90 as a viscosity and bio-adhesive property enhancing agent.

Viscosity

Povidone K 90 is a FDA-approved inactive ingredient (up to 1.2 wt%) for ophthalmic solutions (34) (accessed on December 21 of 2013). MNFs were added with povidone K 90 to optimize a viscosity of ~2.0 centipoise (cP). As these formulations are intended for topical drop administration in the eye, viscosity and bio-adhesive properties of the formulation are critical. Addition of povidone K 90 to MNF resulted in an increased viscosity (see Fig. 1). To deliver rapamycin MNF as topical drop and to hold MNF in the pre-corneal pocket for longer time, an optimal formulation viscosity is preferred. A high viscosity was reported to have an impact on rate of tear drainage (35). Therefore, viscosity for all the MNFs was adjusted to ~2.0 cP. An optimal povidone K 90 weight percentage was 0.6 wt% which demonstrated an easy-flow property to deliver MNF as drops. Also, due to improved formulation viscosity and bio-adhesive properties of povidone K 90,

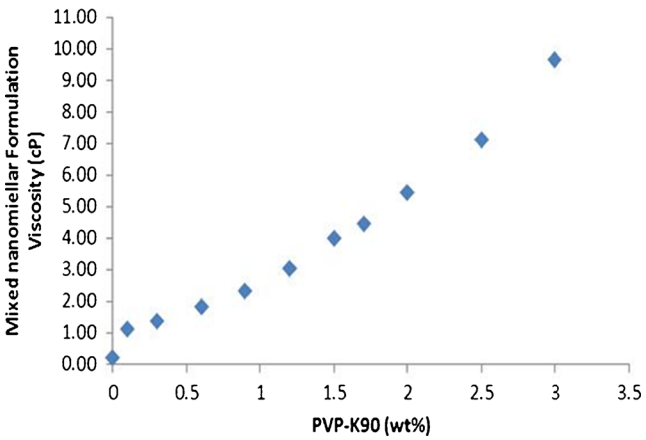

Fig. 1. Effect of increasing PVP-K90 (wt%) on formulation viscosity

MNF may be retained in the pre-corneal pocket for a longer time, reduce tear wash-off, and improve drug delivery.

Osmolality and pH

Topical ophthalmic MNF drops require optimal osmolality and pH to avoid adverse effects on the eye. In general, xylitol, glucose, boric acid, or sodium chloride (NaCl) are added as tonicifiers. Tears have a tonicity equivalent to 0.9% NaCl solution (36) that produces an osmolality of ~300 mOsm/kg. Therefore, ocular formulation osmolality requires to be adjusted in the physiological range. Tear pH ranges between 6.5 and 7.6 (37). Variation in formulation tonicity and pH may cause ocular irritation. Therefore, NaCl was added to MNF and the tonicity was adjusted to 300 mOsm/kg. Similarly, pH of the MNF was adjusted to ~6.8 with 0.1 N sodium hydroxide or hydrochloric acid solution.

Characterization of Mixed Nanomicellar Formulation

Optical Clarity/Appearance

Optical clarity/appearance refers to 90% or greater transmission of light at 400-nm wavelength through a 1.0-cm path length. In general, light scattering occurs when a particle interferes with the visible light wavelength. Due to extreme small nano size of the placebo/blank and rapamycin-loaded MNF, light did not produce any scattering, which denotes a clear/transparent aqueous solution. Rapamycin MNFs are clear with an absorption below 0.05 at 400 nm (Table I). Therefore, this nanomicellar solution is suitable for ophthalmic delivery. Low absorbance of the formulation indicates that MNFs are devoid of any particulate matter. MNF optical clarity was compared to HyClone water which indicated that the placebo and rapamycin-loaded formulations are very similar to water with no particulate matter present.

Entrapment and Loading efficiency

Rapamycin entrapment and loading into MNFs was determined with RP-HPLC method as described previously. All the MNFs showed excellent drug entrapment and loading efficiencies, which are summarized in Table I. All the formulations demonstrated excellent entrapment efficiency. Drug loading enhanced with higher concentrations of rapamycin into MNF.

Size, PDI, and Surface Potential

Mixed nanomicellar size and polydispersity indices were determined for the prepared formulations. Results show a size range between 5 and 20 nm (Table I) for both placebo and rapamycin-loaded MNF (Fig. 2a, b). Polydispersity indices were observed to be less than 0.10. Blank MNF (Vit E TPGS/Oc-40; 4.5:2.0) exhibited an average mixed nanomicellar size of 10.98±0.089 nm. Increasing rapamycin loading did not show any significant difference in size (Table I). Figure 2 represents size distribution for blank and 0.2% rapamycin-loaded MNF. We hypothesize that the size of MNF is sufficiently suitable to traverse across ocular tissues such as scleral channels/pore that have a size range between 20 and 80 nm (38). Also, these micelles display a narrow and unimodal particle size distribution. Since these MNFs are in the same size range as membrane receptors, proteins, and other biomolecules, these carriers may bind and traverse across cellular barriers. Surface charge of MNFs appeared slightly negative (Table I).

Mixed Nanomicelle Surface Morphology

Surface morphology of rapamycin-loaded MNFs was studied with TEM with uranyl acetate as staining agent. This negative staining relies on residual stain remaining on the surface of the mixed nanomicelles such that micelles are clearly defined and visible under TEM. Results revealed that MNFs are spherical in shape with smooth surface architecture and without any signs of aggregation (Fig. 3a). Micelles are clearly defined and distinguished as bright, discrete spherical globules on the TEM grid. The particle size visualized by TEM was in agreement with the size obtained by DLS. The formulation appeared similar to water but shows drug-loaded mixed nanomicelles (Fig. 3b).

^{1}H NMR Studies

^{1}H NMR analysis was applied to identify the drug molecules in solution at parts per million (ppm) levels. In the present study, qualitative ^{1}H NMR spectral analysis was conducted to confirm rapamycin entrapment into the central nanoenvironment of mixed nanomicelles in $CDCl_3$ and D_2O. Placebo and rapamycin-loaded MNFs were prepared in different media such as $CDCl_3$ and D_2O. ^{1}H NMR spectroscopy studies were conducted for rapamycin alone (Fig. 4a), polymer blends in $CDCl_3$ (Fig. 4b), and rapamycin entrapped MNF in $CDCl_3$ and D_2O. Rapamycin entrapped in the MNF is ~800 times higher in concentration than its aqueous solubility (2.6 μg/mL). Generally, addition of such higher concentration of rapamycin in water causes drug precipitation at the bottom of vial due to insolubility. In our preparation, we did not observe any precipitate formation at the bottom of the vial. However, a small amount of unentrapped rapamycin may be present in the outer aqueous environment (D_2O), which may not be identified visually.

Table I. Characteristics of the Mixed Nanomicellar Formulation

Sample	Entrapment efficiency (%)±SD	Loading efficiency (%)±S.D	Micelle size (nm)±SD	Polydispersity index	Surface potential (mV)	Appearance (400 nm)
Placebo	–	–	10.98±0.089	0.08	−0.812	0.036
0.1%	98.3±1.5	1.49±0.02	10.54±0.089	0.07	−0.580	0.042
0.2%	100±1.2	2.99±0.03	10.84±0.11	0.05	−0.789	0.041

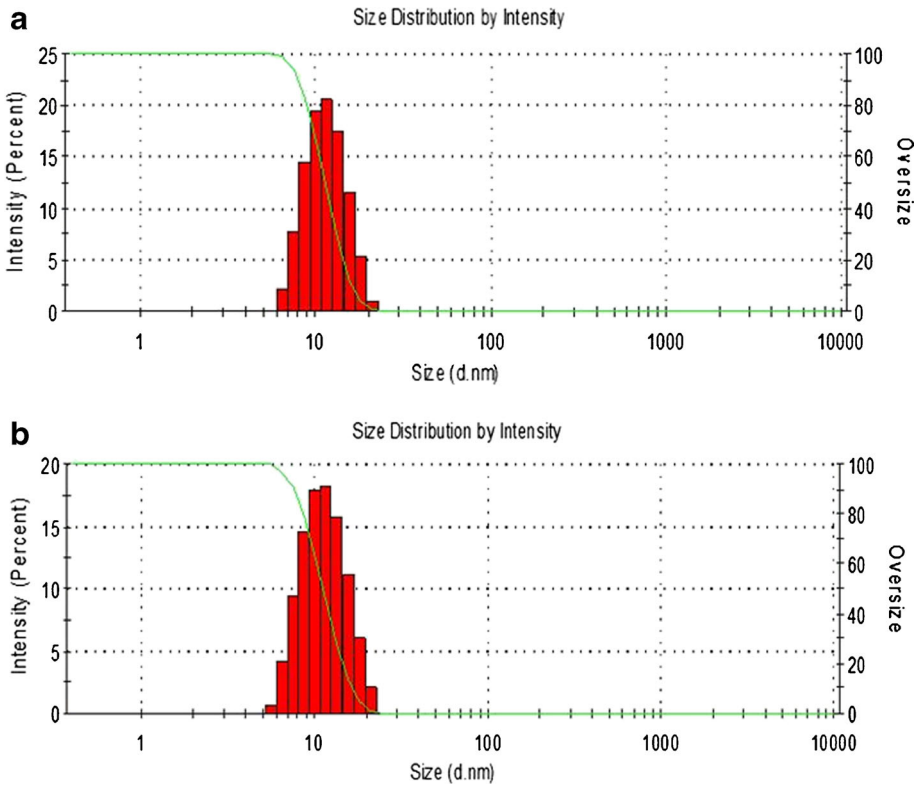

Fig. 2. Mixed nanomicellar size distribution for **a** placebo and **b** 0.2% rapamycin-loaded MNF

Results indicated that in $CDCl_3$, the resonance peaks corresponding to rapamycin and MNFs were present (Fig. 4c). But, in D_2O peaks corresponding to only polymer blends are detected. No peaks corresponding to rapamycin were evident (Fig. 4d). These results clearly indicate that rapamycin was entrapped inside the hydrophobic nanoenvironment/core of mixed nanomicelles. Also, study suggests that no free rapamycin was present in the aqueous MNF. These results are similar to earlier results for paclitaxel-loaded mixed polymeric micelles in D_2O (39,40).

Dilution Stability Studies

Upon topical drop instillation, rapamycin-loaded mixed nanomicelles may be rapidly diluted causing increase in size and release of drug. To study the effect of dilution on the MNF, samples were diluted from 0 to 100 times. The concentration of monomers at these dilutions are well above the CMC. In general, tears are produced at an average flow rate of 1.2 μL/min. Any excessive tear production upon MNF instillation should not have an impact on MNF size. Therefore, we examined the dilution effect on nanomicellar size up to 100-fold dilution (way above tear dilution that is expected *in vivo*). The results of this dilution study are shown in Fig. 5. Mean micelle increased with dilution without any significant impact. The reason may be attributed to decrease in concentration of monomers in the MNF with dilution. Our results are similar to the earlier studies. Xu *et al*. hypothesized that the outer hydrophilic polyethylene oxide segment would form large and loose complex clusters in aqueous solution (41).

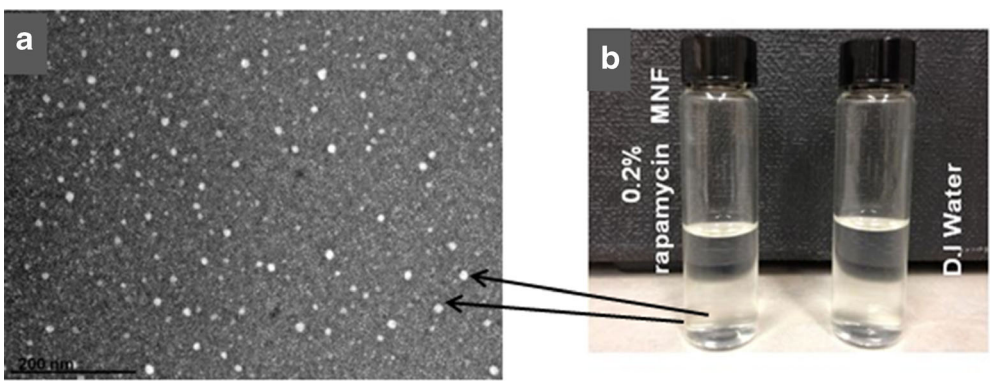

Fig. 3. **a** Real-time scanning transmission electron microscope (STEM) image of 0.2% rapamycin-loaded mixed nanomicellar formulation (×147,000). *Scale bar* 200 nm. **b** Image showing visual appearance 0.2% rapamycin-loaded MNF on the *left side* in comparison to water on the *right side*

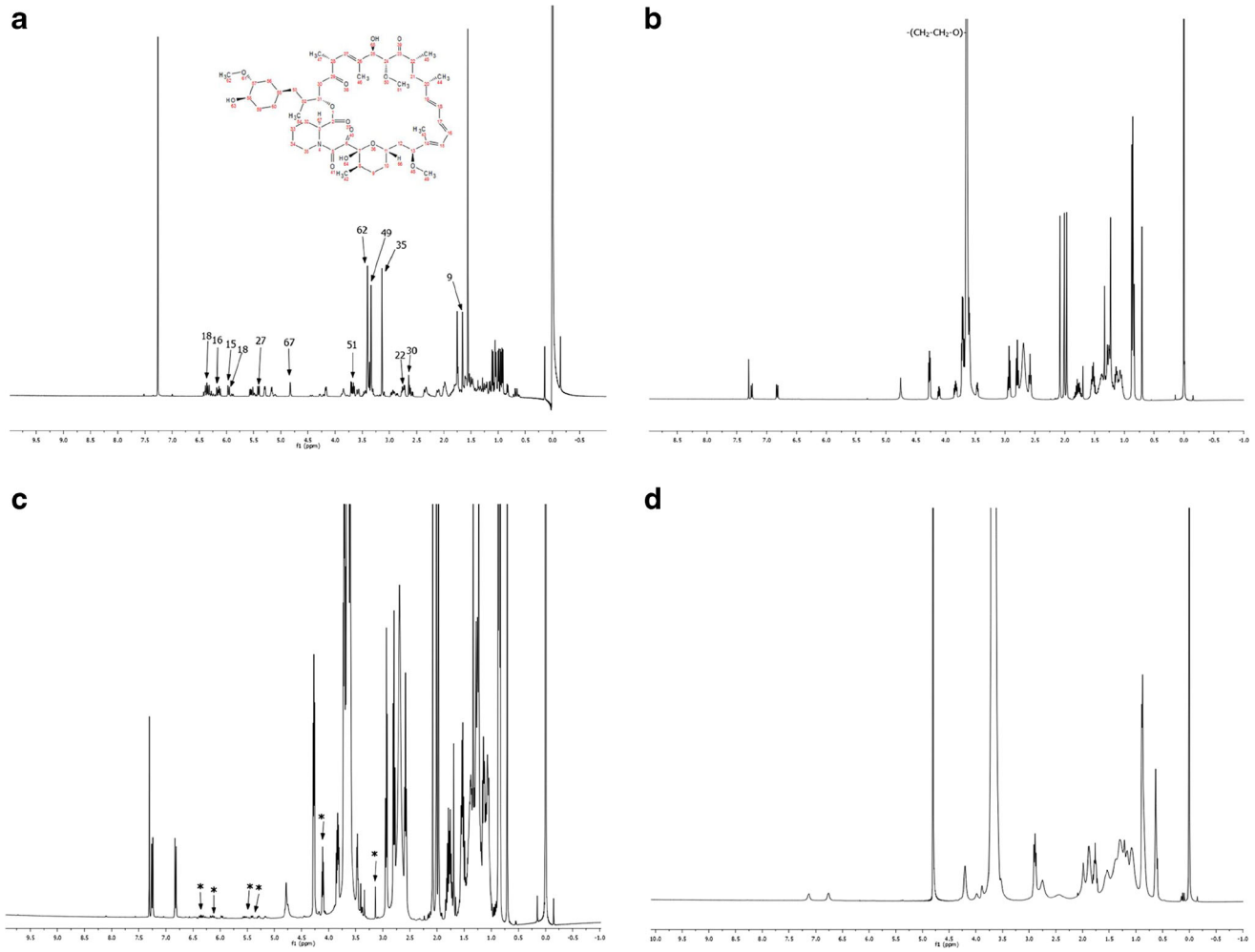

Fig. 4. ^{1}H NMR spectral studies **a** ^{1}H NMR for pure rapamycin in $CDCl_3$. **b** ^{1}H NMR for placebo mixed nanomicelles in $CDCl_3$. **c** ^{1}H NMR for rapamycin-loaded mixed nanomicelles in $CDCl_3$. The symbol *asterisk* indicates the resonance peak for rapamycin. **d** ^{1}H NMR for rapamycin-loaded mixed nanomicelles in dueterated water (D_2O)

These new larger aggregates developed during dilution exhibit thermodynamically reversible association. Hydrophobic effect and hydrogen bonding may force the outer hydrophilic segment to cluster in aqueous solution. Clustering of outer hydrophilic segments may be the reason for increase in micelle size with dilution. The same reason is applicable to our studies. Upon dilution, polymer concentration is lowered which leads to a slight increase in micellar size (41). The prepared mixed nanomicelles in this study sustained the dilution effect on their size and demonstrated negligible effect upon dilution indicating high stability upon dilution.

Cytotoxicity Studies

After topical ophthalmic drop instillation into pre-corneal pocket, formulations/solutions are rapidly cleared (within 5 to 10 min) (6,42). Therefore, to determine the cytotoxic effect of MNF upon long-time exposure to ocular tissues, LDH and cell proliferation assay were performed for 1 and 2 h of exposure. It was assumed that a 1-h incubation period would be sufficient to evaluate any toxicity. Percent rPCEC viable cells for 0.2% rapamycin MNFs were comparable to that of negative control (culture medium) (Fig. 6). Triton-X 100 served as positive control which reduced the percent cell viability to ~30 and ~6% for rPCEC and D407 cells. In another set of studies, cell plasma membrane damage tests (LDH assay) were studied with rPCECs. The amount of LDH released in the culture media directly correlates with membrane damage and cytotoxicity. Triton-X 100 caused significant toxicity/membrane damage. Percentage cytotoxicity to rPCECs post exposure to MNFs (blank and 0.2% rapamycin) for 2 h appeared to be similar to negative control (Fig. 7) indicating MNFs do not cause cell membrane damage. Results from these assays clearly suggest that MNFs are not cytotoxic. Therefore, these formulations appeared to be safe for topical ocular application.

In Vivo Posterior Ocular Tissue Rapamycin Distribution Studies

Delivery of drug to the back-of-the-eye is a major challenge. Diseases affecting the posterior segment ocular tissues, retina-choroid, require long-term drug delivery. To determine whether the developed MNF can deliver the

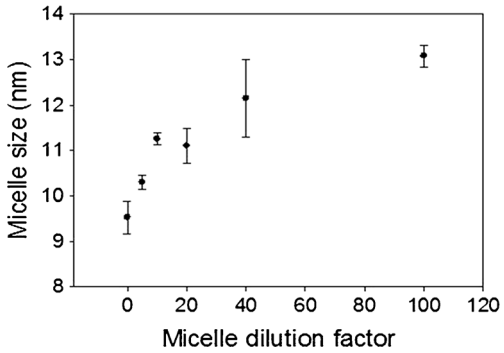

Fig. 5. Effect of dilution on mixed nanomicellar size

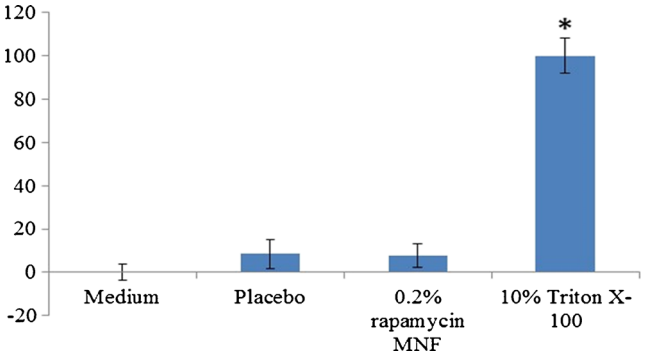

Fig. 7. LDH assay results for placebo and 0.2% rapamycin MNF on rPCECs indicating negligible LDH release upon 2-h MNF exposure. Triton-X 100 (10%) is positive control and culture medium is negative control. A p value of <0.05 was considered significant

hydrophobic rapamycin, to the back-of-the-eye tissues, an *in vivo* ocular tissue distribution study was conducted following topical (0.2% rapamycin) instillation into the pre-corneal pocket of rabbits.

Individual calibration curve were prepared for each ocular tissue and fluid. Multiple reactions monitoring (MRM) mode was utilized to detect the compound of interest. MRM transition for rapamycin m/z [M+Na]+ 936.4/409.3 and for IS (erythromycin) m/z [M+H]+ 734.4/576.5 were optimized (Fig. 8). Specificity and selectivity of the method were tested by analyzing posterior ocular blank tissues and fluid. To assess blank interference with the peak of interest (rapamycin), we processed six replicates at the lower limit of quantification (LLOQ). Peak areas of blanks co-eluting with the analyte was less than 20% of the mean peak area at LLOQ. Intra-day and inter-day precision and accuracy experiments were performed by analyzing extracted calibration curve and QC standards. Accuracy of the method was between 85 and 115% of the nominal value in all the standards, except at the lower limit of quantitation (LLOQ) level, which was 80–120%. Precision was calculated using the coefficient of variation multiplied by 100. Precision of the method was less than 15% of the nominal concentration except at the LLOQ, which was below 20%. The inter-day precision validation was conducted at 3.5, 10, 480, and 800 ng/mL. The LLOQ with inter-day coefficients of variation ranged between 2.3 and 16.7% for sclera, vitreous humor, and retina-choroid. The calibration curve was prepared from 3.5, 10.48, 29.5, 187.2, 312.0, 480, and 800 ng/mL rapamycin doped in respective tissue sample extracts. The lower limit of quantitation (LLOQ) was determined to be 10.48 ng/mL for sclera and vitreous humor. LLOQ for retina-choroid was 3.5 ng/mL with a regression coefficient of 0.9984.

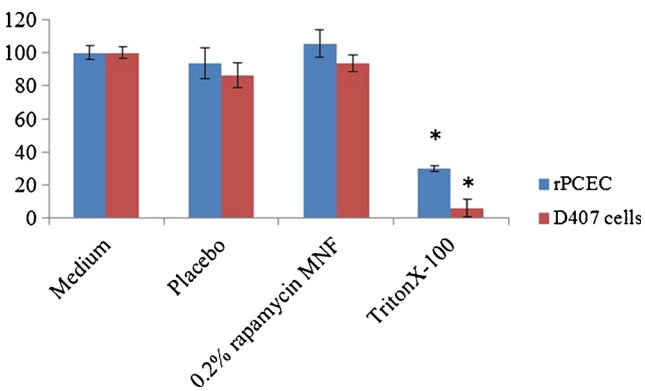

Fig. 6. Cell proliferation assay demonstrating percent cell viability for blank and 0.2% rapamycin MNF on rPCEC and D407 cells after 1-h exposure time. Triton-X 100 (10%) is positive control and culture medium is negative control. A p value of <0.05 was considered significant

Topical drop instillation of 0.2% rapamycin MNF demonstrated detectable and quantifiable rapamycin levels in the back-of-the-eye tissues (sclera and retina-choroid). Rapamycin concentrations quantified in anterior chamber eye tissues (cornea, iris-ciliary body, lens, and aqueous humor) were reported previously (33). We now report rapamycin concentrations in the back-of-the-eye tissues (sclera, retina-choriod) and fluid (vitreous humor) (Table II). *In vivo* ocular tissue distribution studies with single topical drop instillation into rabbit pre-corneal pocket demonstrated detectable levels of rapamycin in the back-of-the-eye tissues. No rapamycin was detected in the vitreous humor. Results indicate that retina-choroid retained the drug at a concentration of 362.35±56.7 ng/g tissue (Table II).

Topically administered drugs may follow corneal and/or conjunctival-scleral pathway to reach the back-of-the-eye tissues (43). Current mode of drug delivery to posterior segment of the eye is primarily by invasive routes like subconjunctival, intravitreal injections, or implants. These methods are also associated with serious complications. Again, this method of drug delivery requires medical specialist to administer the drug, which makes treatment expensive. Also, these drugs are required to be administered for multiple times. Such invasive mode of delivery may provide treatment to back-of-the-eye diseases but may cause serious ocular complications leading to vision loss. Therefore, to overcome such complications, patient compliant formulations like topical drops need to be developed. One of the major drawbacks with topically applied drug formulations is sub-therapeutic levels of drug reaching the back-of-the-eye tissues. To address these problems and replace the current existing route of drug administration to retina-choroid, we have developed patient-compliant clear, aqueous MNF topical drops that could deliver the drug non-invasively to the back-of-the-eye tissues. Most of the potent drug molecules suffer from two major barriers (i) sub-optimal physicochemical properties such as low aqueous solubility and (ii) ocular static and dynamic barriers. Ocular static barriers include sclera, retinal pigment epithelium (RPE), and multi drug-resistance efflux pumps. And, the dynamic barriers

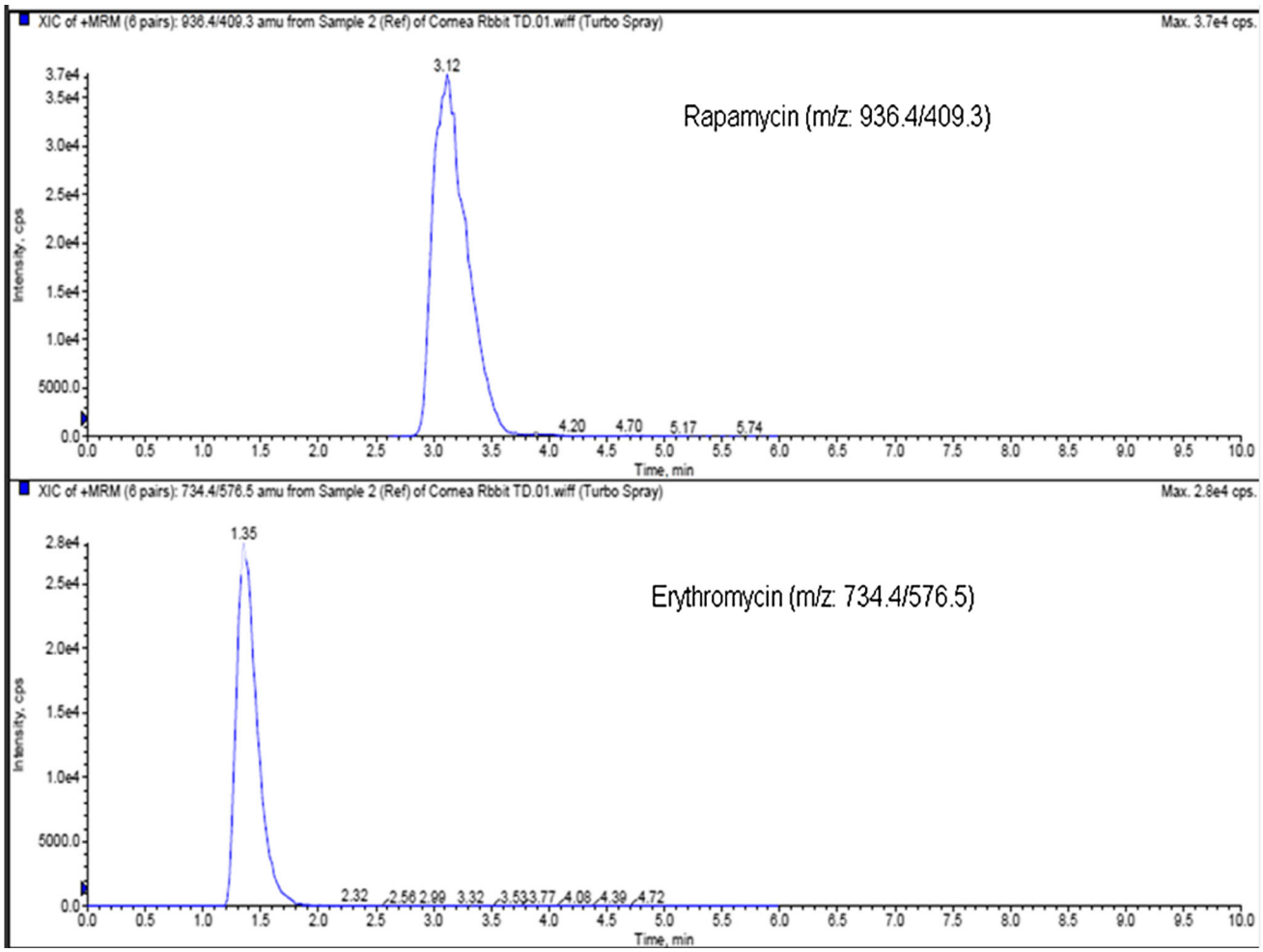

Fig. 8. MRM transition for rapamycin *m*/*z*[M+Na]+ 936.4/409.3, and erthromycin *m*/*z*[M+H]+ 734.4/576.5

include conjunctival and choroidal blood and lymph vessels that wash drug out of ocular tissues into the systemic circulation. Moreover, due to high lipophilicity, rapamycin may not be able to translocate across the cornea (20), which is in agreement with our previously reported results (33).

Non-corneal route may be explored as a predominant route for back-of-the-eye delivery in comparison to corneal route. Aqueous solubility of the molecule is an important determinant for its transport across sclera but also for its ability to evade the conjunctival blood and lymph vessel-mediated washout (44). Scleral aqueous pore diameter varies between 20 and 80 nm (38), which facilitates the diffusion of small hydrophilic molecules. However, rapamycin being highly hydrophobic undergoes partitioning to a larger extent into lipophilic retinal tissue. In current formulation, rapamycin was sequestered into aqueous MNF with improved solubility (~800 times) relative to its aqueous solubility of 2.6 μg/mL (20). At the same time, hydrophilic corona of the nanomicelles can be highly effective in utilizing scleral aqueous channels/pores. This alternative route may help permeation of mixed nanomicelles to reach the back-of-the-eye tissues (retina-choroid). Moreover, highly polar hydrophilic nanomicellar corona may minimize washout into the systemic circulation from the conjunctival and choroidal blood and lymph vessels thus overcoming dynamic barriers. The rapamycin MNF present in sclera may act as a depot and slowly release the drug to

Table II. Posterior Ocular Rapamycin Tissue Drug Concentrations in Rabbits (10 Eyes) After 1 h of Single Topical Dosing (50 μL)

Tissue	0.2% MNF average amount of rapamycin (ng/g of tissue) mean±SEM
Sclera	486.39±89.99
Retina/Choroid	362.35±56.17
Vitreous Humor	ND

LLOQ for retina/choroid=3.5 ng/mL. LLOQ for sclera and vitreous humor=10.48 ng/mL
SEM standard error of mean, *ND* not detectable

deeper ocular tissues. On the other hand, we hypothesize that if the mixed nanomicelles release rapamycin in scleral tissue, a constant rapamycin release to retinal tissues may be achieved which is an added advantage with MNF. MNF can follow the same route of drug transport (transcleral pathway) that was previously observed with sub-conjunctival injection of rapamycin (45).

Mixed nanomicelles in the posterior ocular tissues release rapamycin to highly lipophilic retinal tissues. However, rapamycin molecules do not appreciably partition into hydrophilic vitreous humor as evidenced by non-detectable rapamycin in vitreous humor. Hence, rapamycin accumulates in the lipoidal retinal layers. This drug is a substrate for efflux pumps like P-gp (46,47). Vit E TPGS is found to modulate P-gp efflux transport *via* P-gp ATPase inhibition (48). Upon disruption of micelles and release of rapamycin into the back-of-the-eye lipid tissues, Vit E TPGS monomers may help to inhibit P-gp. Thereby, higher rapamycin accumulation into retina/choroid (Fig. 9) may be achieved. Results from this study suggest that mixed nanomicelles are novel carriers that can overcome both the static and dynamic ocular barriers and deliver therapeutic levels of rapamycin to the back-of-the-eye tissue (retina-choroid). It is noted that much higher than presumably therapeutic levels of rapamycin (7–12 ng/mL) (20) was delivered to retina-choroid with a single topical drop instillation, indicating MNF to be safe and novel carriers for rapamycin.

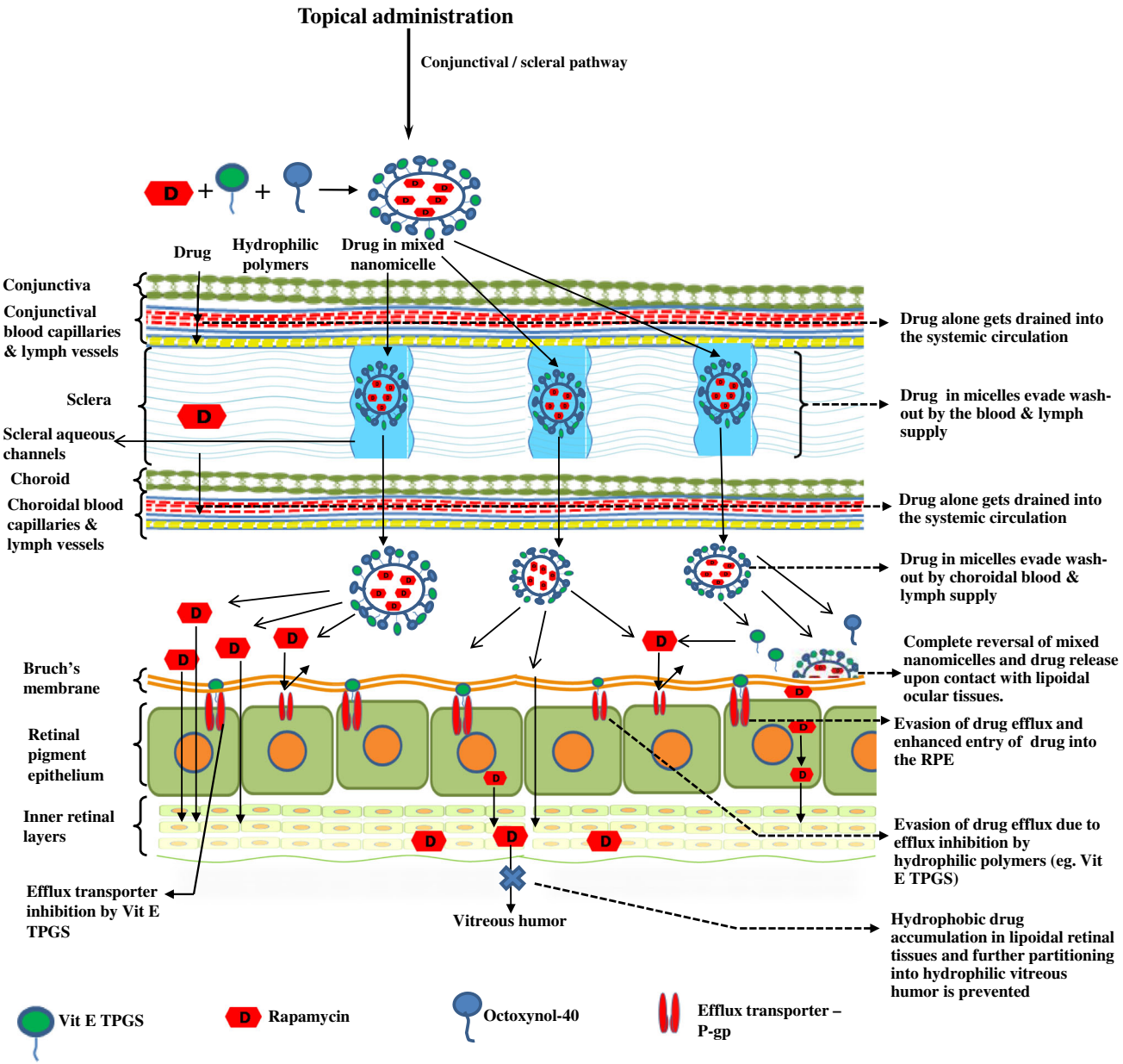

Fig. 9. Hypothetical representation of rapamycin-loaded mixed nanomicelles reaching the back-of-the-eye (retina-choroid) following conjunctival scleral pathway after topical drop administration. Vitamin E tocopherol polyethylene glycol succinate-1000 (Vit E TPGS), P-glycoprotein (P-gp)

CONCLUSIONS

A stable, clear aqueous 0.2% rapamycin-loaded MNF has been prepared and characterized. Rapamycin loading shows excellent entrapment efficiency. Mixed nanomicellar size was found to be ~10 nm with narrow polydispersity index. Surface potential studies demonstrated the formulations to carry slight negative charge. MNF were tested *in vitro* for their cytotoxicity on rPCECs and D407 cells following cell proliferation and LDH assays. Both cell assays demonstrated negligible cytotoxic effect with MNF relative to triton-X 100. Both studies demonstrated that placebo and 0.2% rapamycin-loaded MNF are very safe and tolerable to the eye. *In vivo* ocular tissue distribution studies with single topical drop instillation demonstrated rapamycin to reach retina/choroid. High levels of rapamycin were obtained in retina-choroid measured with sensitive LC-MS/MS. No rapamycin was present in vitreous body. These results indicate that MNF is able to deliver rapamycin to the retina/choroid tissues following topical drop administration to the eye and rapamycin is sequestered into the lipid environment of RPE and Bruch's membrane and does not partition back to the aqueous environment of vitreous humor. Further studies such as *in vivo* pharmacokinetics, ocular safety, and tolerability studies are warranted to determine *in vivo* safety of this novel rapamycin-loaded mixed nanomicellar formulations.

ACKNOWLEDGMENTS

This study was supported by NIH grants R01EY09171-16 and R01EY010659-14. We would like to thank Dr. Vladimir Dusevich, UMKC School of Dentistry, for helping with the operation of transmission electron microscopy. The authors also acknowledge LUX Biosciences, NJ, USA, for the financial support.

REFERENCES

1. Nguyen QD, Ibrahim MA, Watters A, Bittencourt M, Yohannan J, Sepah YJ, *et al.* Ocular tolerability and efficacy of intravitreal and subconjunctival injections of sirolimus in patients with non-infectious uveitis: primary 6-month results of the SAVE Study. J ophthalmic Inflamm Infect. 2013;3(1):32. PubMed PMID: 23514595Pubmed Central PMCID: 3610181.
2. Caspi R. Autoimmunity in the immune privileged eye: pathogenic and regulatory T cells. Immunol Res. 2008;42(1–3):41–50. PubMed PMID: 18629448 Pubmed Central PMCID: 2756228.
3. Gupta R, Murray PI. Chronic non-infectious uveitis in the elderly: epidemiology, pathophysiology and management. Drugs Aging. 2006;23(7):535–58. PubMed PMID: 16930083.
4. Pato E, Munoz-Fernandez S, Francisco F, Abad MA, Maese J, Ortiz A, *et al.* Systematic review on the effectiveness of immunosuppressants and biological therapies in the treatment of autoimmune posterior uveitis. Semin Arthritis Rheum. 2011;40(4):314–23. PubMed PMID: 20656330.
5. Durrani OM, Tehrani NN, Marr JE, Moradi P, Stavrou P, Murray PI. Degree, duration, and causes of visual loss in uveitis. Br J Ophthalmol. 2004;88(9):1159–62. PubMed PMID: 15317708 Pubmed Central PMCID: 1772296.
6. Cholkar K, Patel SP, Vadlapudi AD, Mitra AK. Novel strategies for anterior segment ocular drug delivery. J ocul pharmaco ther J Assoc Ocul Pharmacol Ther. 2013;29(2):106–23. PubMed PMID: 23215539 Pubmed Central PMCID: 3601677.
7. Bian ZM, Elner SG, Elner VM. Regulation of VEGF mRNA expression and protein secretion by TGF-beta2 in human retinal pigment epithelial cells. Exp Eye Res. 2007;84(5):812–22. PubMed PMID: 17331500 Pubmed Central PMCID: 2094015.
8. Khurana RN, Do DV, Nguyen QD. Anti-VEGF therapeutic approaches for diabetic macular edema. Int Ophthalmol Clin. 2009;49(2):109–19. PubMed PMID: 19349791.
9. Kabeel MM, El-Batarny AM, Tameesh MK, Abou El Enein MA. Combined intravitreal bevacizumab and photodynamic therapy with vertiporfin for management of choroidal neovascularization secondary to age-related macular degeneration. Clin Ophthalmol. 2008;2(1):159–66. PubMed PMID: 19668400Pubmed Central PMCID: 2698683.
10. Blumenkranz MS, Woodburn KW, Qing F, Verdooner S, Kessel D, Miller R. Lutetium texaphyrin (Lu-Tex): a potential new agent for ocular fundus angiography and photodynamic therapy. Am J Ophthalmol. 2000;129(3):353–62. PubMed PMID: 10704552.
11. Wu L, Murphy RP. Photodynamic therapy: a new approach to the treatment of choroidal neovascularization secondary to age-related macular degeneration. Curr Opin Ophthalmol. 1999;10(3):217–20. PubMed PMID: 10537782.
12. Stahl A, Paschek L, Martin G, Gross NJ, Feltgen N, Hansen LL, *et al.* Rapamycin reduces VEGF expression in retinal pigment epithelium (RPE) and inhibits RPE-induced sprouting angiogenesis *in vitro*. FEBS Lett. 2008;582(20):3097–102. PubMed PMID: 18703055.
13. Salzmann J, Lightman S. The potential of newer immunomodulating drugs in the treatment of uveitis: a review BioDrugs clinical immunotherapeutics. Biopharmaceuticals gene ther. 2000;13(6):397–408. PubMed PMID: 18034546.
14. Sehgal SN. Rapamune (RAPA, rapamycin, sirolimus): mechanism of action immunosuppressive effect results from blockade of signal transduction and inhibition of cell cycle progression. Clin Biochem. 1998;31(5):335–40. PubMed PMID: 9721431.
15. Terada N, Lucas JJ, Szepesi A, Franklin RA, Domenico J, Gelfand EW. Rapamycin blocks cell cycle progression of activated T cells prior to events characteristic of the middle to late G1 phase of the cycle. J Cell Physiol. 1993;154(1):7–15. PubMed PMID: 8419408.
16. Wong GK, Griffith S, Kojima I, Demain AL. Antifungal activities of rapamycin and its derivatives, prolylrapamycin, 32-desmethylrapamycin, and 32-desmethoxyrapamycin. J antibiotics. 1998;51(5):487–91. PubMed PMID: 9666177.
17. Guba M, von Breitenbuch P, Steinbauer M, Koehl G, Flegel S, Hornung M, *et al.* Rapamycin inhibits primary and metastatic tumor growth by antiangiogenesis: involvement of vascular endothelial growth factor. Nat Med. 2002;8(2):128–35. PubMed PMID: 11821896.
18. Dejneka NS, Kuroki AM, Fosnot J, Tang W, Tolentino MJ, Bennett J. Systemic rapamycin inhibits retinal and choroidal neovascularization in mice. Mol Vis. 2004;10:964–72. PubMed PMID: 15623986.
19. Rouf MA, Vural I, Renoir JM, Hincal AA. Development and characterization of liposomal formulations for rapamycin delivery and investigation of their antiproliferative effect on MCF7 cells. J liposome res. 2009;19(4):322–31. PubMed PMID: 19863167.
20. Buech G, Bertelmann E, Pleyer U, Siebenbrodt I, Borchert HH. Formulation of sirolimus eye drops and corneal permeation studies. J ocul pharmaco ther J Assoc Ocul Pharmacol Ther. 2007;23(3):292–303. PubMed PMID: 17593014.
21. Trepanier DJ, Gallant H, Legatt DF, Yatscoff RW. Rapamycin: distribution, pharmacokinetics and therapeutic range investigations: an update. Clin Biochem. 1998;31(5):345–51. PubMed PMID: 9721433.
22. Yatscoff RW, Wang P, Chan K, Hicks D, Zimmerman J. Rapamycin: distribution, pharmacokinetics, and therapeutic range investigations. Ther Drug Monit. 1995;17(6):666–71. PubMed PMID: 8588238.
23. Zhaoliang Zhang LX, Hao Chen, Xingyi Li. Rapamycin-loaded poly(ε-caprolactone)-poly(ethylene glycol)-poly(ε-caprolactone) nanoparticles: preparation, characterization and potential application in corneal transplantation. Journal of Pharmacy and Pharmacology. In press.

24. Forrest ML, Won CY, Malick AW, Kwon GS. *In vitro* release of the mTOR inhibitor rapamycin from poly(ethylene glycol)-b-poly(epsilon-caprolactone) micelles. J controlled release j Controlled Release Soc. 2006;110(2):370–7. PubMed PMID: 16298448.
25. Mu L, Feng SS. Vitamin E TPGS used as emulsifier in the solvent evaporation/extraction technique for fabrication of polymeric nanospheres for controlled release of paclitaxel (Taxol). J controlled release J Controlled Release Soc. 2002;80(1–3):129–44. PubMed PMID: 11943393.
26. Eva-Maria C, Christiane B, Wempe MF, John H, Lisa N, Edgar KJ, *et al*. Influence of vitamin E TPGS poly(ethylene glycol) chain length on apical efflux transporters in Caco-2 cell monolayers. J Control Release. 2006;111(1–2):35–40.
27. Collnot EM, Baldes C, Wempe MF, Kappl R, Huttermann J, Hyatt JA, *et al*. Mechanism of inhibition of P-glycoprotein mediated efflux by vitamin E TPGS: influence on ATPase activity and membrane fluidity. Mol Pharm. 2007;4(3):465–74. PubMed PMID: 17367162.
28. Khandavilli S, Panchagnula R. Nanoemulsions as versatile formulations for paclitaxel delivery: peroral and dermal delivery studies in rats. J investigative dermatol. 2007;127(1):154–62. PubMed PMID: 16858422.
29. Cholkar K, Hariharan S, Gunda S, Mitra AK. Optimization of dexamethasone mixed nanomicellar formulation. AAPS PharmSciTech. 2014 Jul 1. PubMed PMID: 24980081
30. Vadlapudi AD, Cholkar K, Vadlapatla RK, Mitra AK. Aqueous nanomicellar formulation for topical delivery of biotinylated lipid prodrug of acyclovir: formulation development and ocular biocompatibility. Journal of ocular pharmacology and therapeutics : the official journal of the Association for Ocular Pharmacology and Therapeutics. 2013 Nov 5. PubMed PMID: 24192229
31. Hariharan S, Minocha M, Mishra GP, Pal D, Krishna R, Mitra AK. Interaction of ocular hypotensive agents (PGF2 alpha analogs-bimatoprost, latanoprost, and travoprost) with MDR efflux pumps on the rabbit cornea. J ocul pharmaco ther J Assoc Ocul Pharmacol Ther. 2009;25(6):487–98. PubMed PMID: 20028257Pubmed Central PMCID: 3096535.
32. Dong XY, Feng XD, Sun Y. His-tagged protein purification by metal-chelate affinity extraction with nickel-chelate reverse micelles. Biotechnol Prog. 2010;26(4):1088–94. PubMed PMID: 20730766.
33. Earla R, Cholkar K, Gunda S, Earla RL, Mitra AK. Bioanalytical method validation of rapamycin in ocular matrix by QTRAP LC-MS/MS: application to rabbit anterior tissue distribution by topical administration of rapamycin nanomicellar formulation. J Chromatogr B Anal Technol Biomed Life Sci. 2012;908:76–86. PubMed PMID: 23122404Pubmed Central PMCID: 3597233.
34. accessed on December, 21 of 2013. Available from: http://www.accessdata.fda.gov/scripts/cder/iig/getiigWEB.cfm.
35. Zhu H, Chauhan A. Effect of viscosity on tear drainage and ocular residence time. Optometry and vision science American Academy of Optometry. 2008;85(8):715–25. PubMed PMID: 18677227.
36. Benjamin WJ, Hill RM. Tonicity of human tear fluid sampled from the cul-de-sac. Br J Ophthalmol. 1989;73(8):624–7. PubMed PMID: 2765441Pubmed Central PMCID: 1041831.
37. Abelson MB, Udell IJ, Weston JH. Normal human tear pH by direct measurement. Arch Ophthalmol. 1981;99(2):301. PubMed PMID: 7469869.
38. Chopra P, Hao J, Li SK. Iontophoretic transport of charged macromolecules across human sclera. Int J Pharm. 2010;388(1–2):107–13. PubMed PMID: 20045044Pubmed Central PMCID: 2838613.
39. Wei Z, Hao J, Yuan S, Li Y, Juan W, Sha X, *et al*. Paclitaxel-loaded Pluronic P123/F127 mixed polymeric micelles: formulation, optimization and *in vitro* characterization. Int J Pharm. 2009;376(1–2):176–85. PubMed PMID: 19409463.
40. Lee SC, Huh KM, Lee J, Cho YW, Galinsky RE, Park K. Hydrotropic polymeric micelles for enhanced paclitaxel solubility: *in vitro* and *in vivo* characterization. Biomacromolecules. 2007;8(1):202–8. PubMed PMID: 17206808Pubmed Central PMCID: 2532792.
41. Renliang Xu MAW, Hallett FR, Gerard R, Croucher MD. Light-scattering study of the association behavior of styrene-ethylene oxide block copolymers in aqueous solution. Macromolecules. 1991;24(1):87–93.
42. Kristiina Järvinena TJ. Arto urtti. Ocular absorption following topical delivery Adv Drug Deliv Rev. 1995;16(1):3–19.
43. Hughes PM, Oleinik O, Joan-En Chang L, Wilson CG. Topical and systemic drug delivery to the posterior segments. Adv Drug Deliv Rev. 2005;57(14):2010–32.
44. Aydemir O, Celebi S, Yilmaz T, Yekeler H, Kukner AS. Protective effects of vitamin E forms (alpha-tocopherol, gamma-tocopherol and d-alpha-tocopherol polyethylene glycol 1000 succinate) on retinal edema during ischemia-reperfusion injury in the guinea pig retina. Int Ophthalmol. 2004;25(5–6):283–9. PubMed PMID: 16532291.
45. Dugel PU. Sirolimus in treatment of retinal diseases. Retina today. 2009 (October):38–41.
46. Anglicheau D, Pallet N, Rabant M, Marquet P, Cassinat B, Meria P, *et al*. Role of P-glycoprotein in cyclosporine cytotoxicity in the cyclosporine-sirolimus interaction. Kidney Int. 2006;70(6):1019–25. PubMed PMID: 16837925.
47. accessed on 31st December 2013. Available from: http://www.fda.gov/drugs/developmentapprovalprocess/developmentresources/druginteractionslabeling/ucm093664.htm.
48. Collnot EM, Baldes C, Schaefer UF, Edgar KJ, Wempe MF, Lehr CM. Vitamin E TPGS P-glycoprotein inhibition mechanism: influence on conformational flexibility, intracellular ATP levels, and role of time and site of access. Mol Pharm. 2010;7(3):642–51. PubMed PMID: 20205474.